AMERICAN SOCIETY FOR MICROBIOLOGY | Journal of Bacteriology®

RESEARCH ARTICLE

Regulation of Polyhydroxybutyrate Accumulation in *Sinorhizobium meliloti* by the *Trans*-Encoded Small RNA MmgR

Antonio Lagares, Jr.,[a,b] Germán Ceizel Borella,[a] Uwe Linne,[c] Anke Becker,[b] Claudio Valverde[a]

Laboratorio de Bioquímica, Microbiología e Interacciones Biológicas en el Suelo, Departamento de Ciencia y Tecnología, Universidad Nacional de Quilmes-CONICET, Bernal, Argentina[a]; LOEWE Center for Synthetic Microbiology and Faculty of Biology, Philipps University Marburg, Marburg, Germany[b]; Faculty of Chemistry-Mass Spectrometry, Phillips University Marburg, Marburg, Germany[c]

ABSTRACT Riboregulation has a major role in the fine-tuning of multiple bacterial processes. Among the RNA players, *trans*-encoded untranslated small RNAs (sRNAs) regulate complex metabolic networks by tuning expression from multiple target genes in response to numerous signals. In *Sinorhizobium meliloti*, over 400 sRNAs are expressed under different stimuli. The sRNA MmgR (standing for Makes more granules Regulator) has been of particular interest to us since its sequence and structure are highly conserved among the alphaproteobacteria and its expression is regulated by the amount and quality of the bacterium's available nitrogen source. In this work, we explored the biological role of MmgR in *S. meliloti* 2011 by characterizing the effect of a deletion of the internal conserved core of *mmgR* (*mmgR*$^{\Delta 33-51}$). This mutation resulted in larger amounts of polyhydroxybutyrate (PHB) distributed into more intracellular granules than are found in the wild-type strain. This phenotype was expressed upon cessation of balanced growth owing to nitrogen depletion in the presence of surplus carbon (i.e., at a carbon/nitrogen molar ratio greater than 10). The normal PHB accumulation was complemented with a wild-type *mmgR* copy but not with unrelated sRNA genes. Furthermore, the expression of *mmgR* limited PHB accumulation in the wild type, regardless of the magnitude of the C surplus. Quantitative proteomic profiling and quantitative reverse transcription-PCR (qRT-PCR) revealed that the absence of MmgR results in a posttranscriptional overexpression of both PHB phasin proteins (PhaP1 and PhaP2). Together, our results indicate that the widely conserved alphaproteobacterial MmgR sRNA fine-tunes the regulation of PHB storage in *S. meliloti*.

IMPORTANCE High-throughput RNA sequencing has recently uncovered an overwhelming number of *trans*-encoded small RNAs (sRNAs) in diverse prokaryotes. In the nitrogen-fixing alphaproteobacterial symbiont of alfalfa root nodules *Sinorhizobium meliloti*, only four out of hundreds of identified sRNA genes have been functionally characterized. Thus, uncovering the biological role of sRNAs currently represents a major issue and one that is particularly challenging because of the usually subtle quantitative regulation contributed by most characterized sRNAs. Here, we have characterized the function of the broadly conserved alphaproteobacterial sRNA gene *mmgR* in *S. meliloti*. Our results strongly suggest that *mmgR* encodes a negative regulator of the accumulation of polyhydroxybutyrate, the major carbon and reducing power storage polymer in *S. meliloti* cells growing under conditions of C/N overbalance.

KEYWORDS MmgR, PHB, riboregulation, *Sinorhizobium meliloti*, small RNA

Received 3 November 2016 **Accepted** 31 January 2017

Accepted manuscript posted online 6 February 2017

Citation Lagares A, Jr, Borella GC, Linne U, Becker A, Valverde C. 2017. Regulation of polyhydroxybutyrate accumulation in *Sinorhizobium meliloti* by the *trans*-encoded small RNA MmgR. J Bacteriol 199:e00776-16. https://doi.org/10.1128/JB.00776-16.

Editor Richard L. Gourse, University of Wisconsin—Madison

Address correspondence to Claudio Valverde, cvalver@unq.edu.ar.

Rhizobia are alpha- and betaproteobacteria capable of establishing symbiotic interactions with leguminous plant roots, where they induce a *de novo* formation of root organs called nodules and after colonization subsequently differentiate into bacteroid cells devoted to carrying out biological nitrogen fixation (BNF) (1, 2). *Sinorhizobium meliloti* is a soil-dwelling alphaproteobacterium able to establish N_2-fixing root nodule symbiosis with legumes from the genera *Medicago*, *Melilotus*, and *Trigonella* (3, 4). The beneficial association between *S. meliloti* and alfalfa (*Medicago sativa*) plant roots represents a reference model for studying the interactions between symbiotic bacteria and the plant host (5). This partnership involves a complex signal exchange between the symbionts that commits them to a joint differentiation process involving biochemical and morphological changes that terminate in the formation of the mature N_2-fixing root nodule (5–7). This remarkably complex interplay has been shown to be tightly regulated at multiple levels in both partners (5, 6).

Extracellular carbon polymers like succinoglycan and galactoglucan are well-known critical elements involved in the root hair infection process, whereas the surface lipopolysaccharide (LPS) is required for proper differentiation of *S. meliloti* into nitrogen-fixing bacteroids within root nodule cells (5). *S. meliloti* can also accumulate intracellular carbon polymers such as glycogen and polyhydroxybutyrate (PHB), notably under growth-limiting conditions (8). PHB appears to be critical for N_2 fixation in young developing *M. sativa* nodules, and glycogen synthesis is essential for N_2 fixation in mature *M. sativa* nodules (9). In free-living *S. meliloti* cells, PHB accumulates when C availability exceeds that of other major nutrients such as N (i.e., at a C/N molar ratio greater than 10) (8) and/or when the cells have excess reducing capacity and need to regenerate NAD(P)H (10). Thus, PHB is a storage compound for both C and reducing power that also confers long-term persistence under starvation conditions (11). In contrast, the role of glycogen in free-living cells remains obscure. The carbon flux between the two intracellular C storage compounds of *S. meliloti* seems to be under transcriptional control by the product of the *aniA* gene (12).

Gene expression in bacteria has been historically associated almost exclusively with the activity of protein regulators that switch on or off transcription; however, during the last 2 decades extensive research has highlighted the roles that untranslated *trans*-encoded small RNA molecules (sRNAs) play as regulators of diverse physiological processes, e.g., cell cycle control, amino acid uptake and metabolism, quorum sensing, iron metabolism and the osmotic stress response, among others, mostly at the post-transcriptional level (13, 14).

S. meliloti has been shown to express more than 400 different sRNAs under different growth conditions and lifestyles, i.e., both free-living in the soil and symbiotically associated in a plant (15–21). In addition, *S. meliloti* expresses a functional homolog of the *Escherichia coli* Hfq protein, a chaperone of RNA-RNA interactions and a modulator of RNA activity (22–29). Nevertheless, the biological implications of the large *S. meliloti* RNome remain largely unexplored (20), since only four small RNAs have been functionally characterized so far, i.e., the cell cycle regulator sRNA EcpR1 (30), the quorum-sensing regulator sRNA RcsR1 (31), and the tandemly encoded orthologs AbcR1 and AbcR2 (32). We are tempted to speculate that the large regulatory network is yet to be revealed.

In this work, we aimed at elucidating the biological role of a particular *trans*-encoded sRNA, which we have originally identified as a transcript of unknown function encoded in the *SMc04042-SMc04043* intergenic region of *S. meliloti* 2011 (19). For reasons that will become clear below, we have renamed this sRNA gene *mmgR* (it was formerly designated *sm8*). The encoded transcript MmgR belongs to the subfamily of orthologous sRNAs αr8s1, which is widely distributed within the alphaproteobacteria and whose members bear a highly conserved sequence and structure in the internal nucleotide core and share microsynteny with their flanking genes (33). The conservation implies there may be a shared, conserved function for *mmgR* homologs; however, to date none have been characterized in other alphaproteobacteria. MmgR is a non-coding 77-nucleotide (nt) transcript (16, 17, 19) that binds to and is stabilized by Hfq

(25, 27). Under symbiotic conditions, MmgR transcripts have been found to be more abundant in the N_2-fixing mature bacteroids of nodule zone III (21). In free-living *S. meliloti* cells, MmgR expression is modulated in response to the quality and amount of the available N source, reaching the highest intracellular level with nitrate as the N source or upon starvation of the organic N sources (34). Here, we report that *S. meliloti* MmgR sRNA acts as a fine-tuning negative regulator of polyhydroxybutyrate (PHB) storage under conditions of N starvation and C surplus.

RESULTS

Construction and validation of an isogenic *mmgR*$^{\Delta 33-51}$mutant of *S. meliloti* 2011. Our objective was to generate an *S. meliloti* 2011 isogenic mutant strain lacking the MmgR transcript. For that purpose, the region carrying *mmgR* was first inspected to prevent introducing nucleotide changes that could affect the expression of the flanking genes, namely, *SMc04042* and *SMc04043*. The recent annotation of transcriptional start sites in the *S. meliloti* 2011 genome (16) allowed us to delimit a safe region in which the risk of introducing polar mutations was minimized. Unfortunately, the complete deletion of the *mmgR* gene was not possible because of its partial overlap with the farthest promoter elements of the upstream and divergently transcribed gene *SMc04042*; we instead targeted an internal and conserved 18-nt core sequence of *mmgR* in order to perform an allelic exchange with a 12-nt unrelated sequence (Fig. 1a). The mutant transcript MmgR$^{\Delta 33-51}$ was predicted to have a modified RNA secondary structure but to retain the Rho-independent terminator to ensure transcription termination (Fig. 1b and c). Expression of the mutant sRNA was analyzed during the stationary phase of growth in *Rhizobium* defined medium (RDM), a condition previously reported to induce the highest intracellular MmgR levels in the wild-type strain (19, 25). The cellular level of MmgR$^{\Delta 33-51}$ RNA in the *mmgR*$^{\Delta 33-51}$ mutant was below the detection limit of a Northern blot assay targeting the 5′ sequence shared in common with the wild-type sRNA (see Fig. 3c). Quantitative reverse transcription-PCR (qRT-PCR)-based expression analysis of the flanking gene *SMc04042* demonstrated that the introduction of the *mmgR*$^{\Delta 33-51}$ mutation did not significantly influence the abundance of *SMc04042* mRNA [$\log_2$ (abundance in *mmgR*$^{\Delta 33-51}$/abundance in wild type) $= -0.4 \pm 0.1$], thus eliminating the possibility of a polarity in the *mmgR*$^{\Delta 33-51}$ allele over the expression of *SMc04042*. Together, these results validated the usefulness of the *S. meliloti* 2011 isogenic *mmgR*$^{\Delta 33-51}$ strain in studying the effect caused by lowering the MmgR transcript level.

MmgR limits PHB accumulation under conditions of N limitation and C surplus. Initially, we compared the growth behaviors (optical density at 600 nm [OD_{600}]) of the wild-type and *mmgR*$^{\Delta 33-51}$ mutant strains in RDM (C/N molar ratio = 30:1). Although the strains displayed a similar growth performance during the exponential phase, the mutant strain was associated with a higher OD_{600} than the wild type after leaving the balanced-growth phase (Fig. 2a). However, we detected no differences in terms of viable cell counts between the wild-type and *mmgR*$^{\Delta 33-51}$ strains (Fig. 2a). As the OD_{600} measurements were done after washing and resuspending the cells in saline solution, these results ruled out the possibility of interference by optically active substances in the culture supernatant and furthermore suggested that the mutation in *mmgR* might cause changes in cell biomass that would be reflected in the OD_{600} values of the *mmgR*$^{\Delta 33-51}$ culture (35). As expected for a phenotype resulting primarily from changes in intracellular MmgR activity, the differential behavior in terms of OD_{600} progression between the strains became evident at the point in the growth curve when the *mmgR* promoter was naturally turned on in the wild-type background (i.e., at the end of the exponential phase of growth), which in turn leads to a large increase in the cellular sRNA transcript level, as we have reported elsewhere (34).

In order to explore the cellular basis of the observed differential OD_{600} yield after exit from the exponential growth phase (Fig. 2a), we determined the cell dry weight of the wild-type *S. meliloti* 2011 and *mmgR*$^{\Delta 33-51}$ strains in the stationary phase of growth in RDM. The *mmgR*$^{\Delta 33-51}$ mutant cells were, on an average, 20% heavier than those of

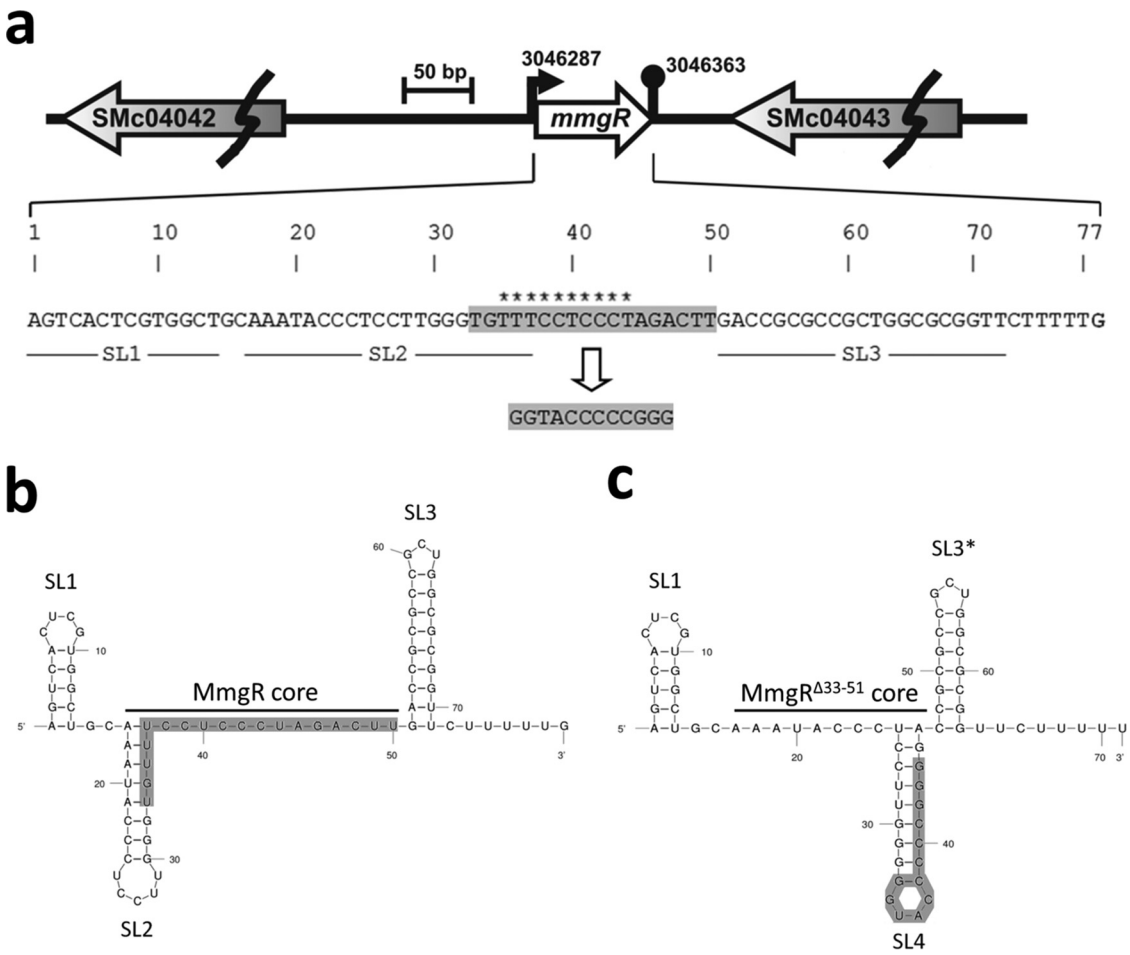

FIG 1 Partial sequence exchange at the internal conserved core of *mmgR* and the predicted impact on the secondary structure of MmgR. (a) The *mmgR* locus and scheme of the mutational approach that was followed to construct the *mmgR*$^{\Delta 33-51}$ allele. The asterisks indicate the fully conserved positions revealed by multiple-sequence alignment of homologous alphaproteobacterial sequences performed previously (33). (b and c) Secondary structure predicted with the Mfold server (70) for the MmgR (b) and MmgR$^{\Delta 33-51}$ (c) sRNAs. The sequence replaced in the wild-type sRNA and the sequence introduced in the mutant MmgR$^{\Delta 33-51}$ sRNA are highlighted in gray. The asterisk indicates that the corresponding mutant stem-loop (SL) structure is predicted to be shorter than that of the wild type.

the wild-type bacteria (Fig. 3a), whereas no significant differences in the protein content per cell of either strain were observed under the same physiological condition (Fig. 3a). This difference suggested that the higher biomass of the *mmgR*$^{\Delta 33-51}$ mutant might be related to a disproportionate accumulation of some storage compound that was not accompanied by a balanced synthesis of the rest of the cellular components.

Considering that the cessation of the exponential phase of growth represents a metabolic status in which synthesis of the C storage polymer PHB had been described to be turned on in rhizobia (8), we explored whether or not a differential accumulation of PHB could be responsible for the observed differences in the average cellular biomass of the two strains under that growth condition. The results indicated that the *mmgR*$^{\Delta 33-51}$ strain did, in fact, accumulate over 20% more PHB than the wild-type strain (Fig. 3a). Furthermore, despite the difference between the geometric mean values for the cellular PHB content of each population, both distributions were unimodal, thus eliminating the possibility of a phenotypic heterogeneity (Fig. 3d; see Fig. S2 in the supplemental material). No difference in the amount of intracellular glycogen as a form of C storage was detected as a result of the mutation of *mmgR* (Fig. 3a).

A genetic complementation of the *mmgR*$^{\Delta 33-51}$ mutant strain through expression of the MmgR sRNA from an inducible copy carried in plasmid pSRK-MmgR (Fig. 3c; see Fig.

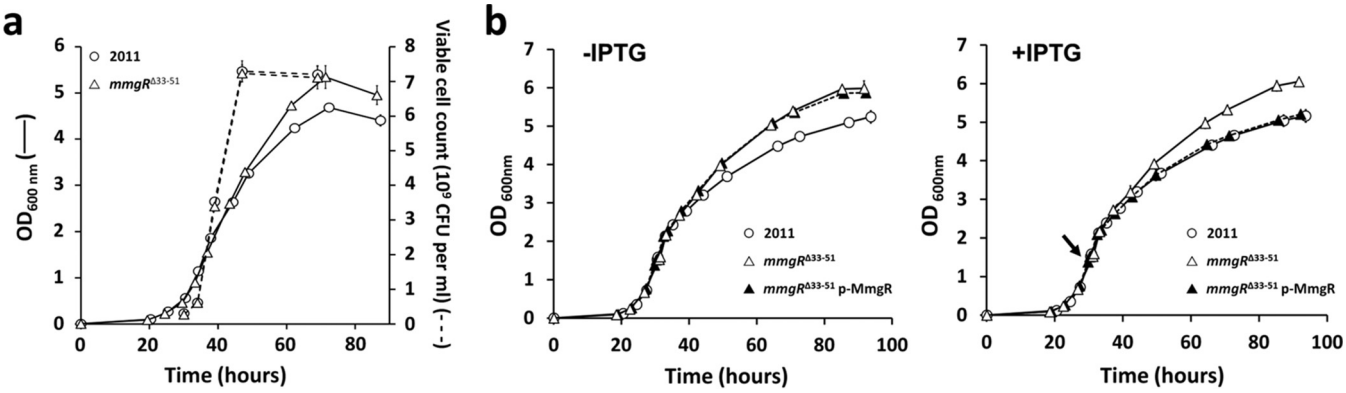

FIG 2 Differential growth yield (OD_{600}) between *S. meliloti* 2011 wild-type and *mmgR*$^{\Delta 33-51}$ mutant strains at the stationary phase of growth in RDM. (a) ○, *S. meliloti* 2011 wild-type strain; △, *S. meliloti* 2011 *mmgR*$^{\Delta 33-51}$ strain. Curves with solid or dashed lines represent the culture optical density at 600 nm (OD_{600}) or viable cell count kinetics, respectively. Each curve represents the average from three independent cultures ± SD. The experiment was repeated three times with essentially the same results. (b) OD_{600} kinetics of cultures in which IPTG was added at an OD_{600} of 1.6 (right panel) and of noninduced cultures (left panel). The arrow indicates the time point at which IPTG was added to the cultures. 2011, wild-type strain. Each curve represents the average from three independent cultures ± SD. The error bars corresponding to SD values lower than 0.1 OD_{600} unit might not be visible in the plot. The experiment was repeated twice with essentially the same results.

S1 in the supplemental material) fully restored the wild-type behavior (Fig. 2b and 3b). In order to mimic the expression pattern of the *mmgR* gene in the wild-type strain (34) during the mutant complementation assay, a plasmid-borne copy of the *mmgR* locus was induced with 500 μM isopropyl-β-D-thiogalactopyranoside (IPTG) once the cultures reached an OD_{600} of 1.6 (Fig. 2b). As expected, neither overexpression of either the Hfq-independent unrelated antisense RNA asRNA812 or the Hfq-dependent sRNA Sm84 (27) nor induction of the mutant allele *mmgR*$^{\Delta 33-51}$ restored the wild-type levels of PHB during the stationary phase within the *mmgR*$^{\Delta 33-51}$ genetic background (Fig. 3b).

To test the hypothesis that the role of MmgR is to control utilization of the C surplus upon the cessation of balanced growth, we evaluated the effect of doubling the C availability in the culture medium on biomass production by the wild-type *S. meliloti* 2011 and the isogenic *mmgR*$^{\Delta 33-51}$ mutant. In the wild-type strain, the higher C availability in the culture medium (C/N ratio, 60:1) did not result in an increased accumulation of biomass, whereas the *mmgR*$^{\Delta 33-51}$ cultures exhibited an even higher biomass production than had been observed during growth in RDM (C/N ratio, 30:1), as revealed by their higher OD_{600} in the stationary phase (Fig. 4a). Measurements of the amounts of intracellular PHB in stationary wild-type and *mmgR*$^{\Delta 33-51}$ bacteria under these growth conditions thus further supported the existence of an uncontrolled accumulation of PHB with an increased C availability in the absence of the MmgR gene product (Fig. 4b).

The observation of stationary-phase wild-type and *mmgR*$^{\Delta 33-51}$ cells growing in RDM by transmission electronic microscopy (TEM) revealed profound morphological and ultrastructural differences between the strains. First, *mmgR*$^{\Delta 33-51}$ cells presented a statistically significant 20% higher length/width ratio (2.33 ± 0.12; $n = 122$; $P < 0.05$) than the wild-type bacteria (1.91 ± 0.05; $n = 82$) (Fig. 5). In addition, the mutant cells displayed a higher number of smaller and morphologically heterogeneous cytoplasmic PHB granules per cell than the wild type (with 3 to 6 well-defined granules per cell on average) (Fig. 5). As expected, exponential-phase cells growing in RDM did not show any such PHB granules in their cytoplasm (Fig. 5).

Higher accumulation of the granule-associated phasin PhaP2 in the *mmgR*$^{\Delta 33-51}$ mutant as revealed by SDS-PAGE followed by mass spectrometry (MS). With an aim of shedding light on the molecular changes underlying the physiological phenotype of the *mmgR*$^{\Delta 33-51}$ mutant, we initially performed a semiquantitative differential proteomic profiling of the wild-type and *mmgR*$^{\Delta 33-51}$ strains at stationary phase in RDM. Total protein extracts from each strain were prepared, and the proteins were separated by 15% (wt/vol) SDS-PAGE. A single band corresponding to

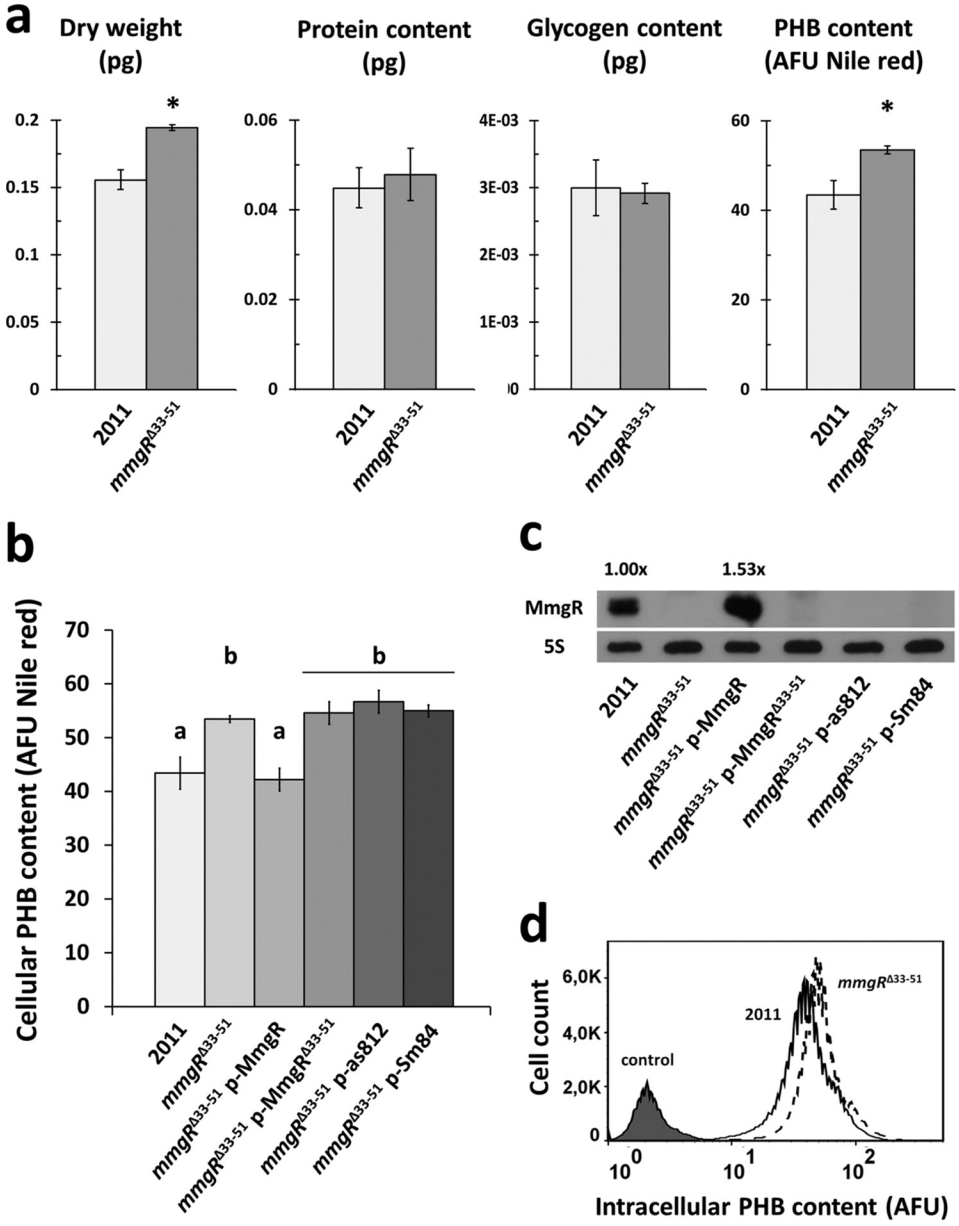

FIG 3 Accumulation of higher PHB levels in the *mmgR*$^{\Delta 33-51}$ strain than in the wild-type strain during the stationary phase of growth under C/N overbalance in RDM. (a) Cellular dry weight and cellular protein, glycogen, and PHB contents of wild-type and *mmgR*$^{\Delta 33-51}$ cells at the stationary phase of growth. The results are the average of the data from three independent cultures ± SD. The asterisk indicates that the average value for the *mmgR*$^{\Delta 33-51}$ strain differs significantly from that for the wild-type strain at a *P* value of <0.05. (b) Cellular PHB contents (arbitrary fluorescence units [AFU]) of the wild-type, *mmgR*$^{\Delta 33-51}$, and *mmgR*$^{\Delta 33-51}$ p-sRNA complemented strains at the stationary phase of growth, as determined by flow cytometric analysis with Nile red as a PHB fluorescent stain. Induction with IPTG of the complemented strains was carried out with cultures having an OD_{600} of 1.6. The results are the average of the data from three independent cultures ± SD. The values were analyzed statistically by Tukey's multiple-comparison test. Different letters over the bars indicate that the average values differ significantly at a *P* value of <0.05. The experiment was repeated twice with essentially the same results. (c) Northern blot analysis confirming that the MmgR level in the *mmgR*$^{\Delta 33-51}$ p-MmgR strain is restored to nearly wild-type levels in the stationary growth phase (after 90 h of growth) after IPTG addition at an OD_{600} of 1.6 (after ca. 30 h of growth). The relative abundance of MmgR (normalized to the signal for the 5S rRNA) in the *mmgR*$^{\Delta 33-51}$ p-MmgR strain relative to that in the wild-type strain is indicated over the image. (d) Frequency distribution of the intracellular PHB contents of *S. meliloti* 2011 (solid line) and *mmgR*$^{\Delta 33-51}$ (dashed line) cells at the stationary growth phase in RDM (C/N ratio, 30:1). Stationary *S. meliloti* 2011 cells in RDM with a balanced C/N ratio (10:1) were used as a negative control for PHB accumulation (shaded histogram). The effect of induction of plasmid-borne MmgR, MmgR$^{\Delta 33-51}$, asRNA812, and Sm84 over the frequency of intracellular PHB content in an *mmgR*$^{\Delta 33-51}$ background is shown in Fig. S2 in the supplemental material.

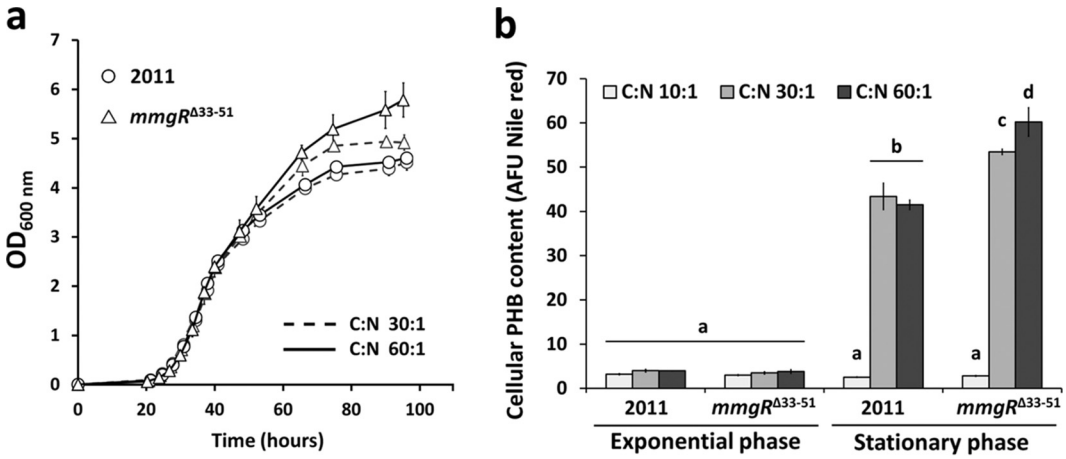

FIG 4 Limitation of PHB accumulation under conditions of N starvation and surplus C set by the expression of MmgR in *S. meliloti*. (a) ○, *S. meliloti* 2011 wild-type strain; △, *S. meliloti* 2011 *mmgR*$^{\Delta 33-51}$ strain. Curves with solid lines or dashed lines represent the OD_{600} kinetics of cultures performed in RDM with a 6× (C/N ratio, 60:1) or a 3× (C/N ratio, 30:1) overbalanced C/N ratio, respectively. Each curve represents the average from three independent cultures ± SD. (b) Cellular PHB content (arbitrary fluorescence units [AFU]) of bacteria in the exponential and stationary growth phases under balanced (10:1) or 3× (30:1) and 6× (60:1) overbalanced C/N ratios. PHB was determined by flow cytometry with Nile red as the PHB fluorescent stain. The results are the average of the data from three independent cultures ± SD. The values were analyzed statistically by Tukey's multiple-comparison test. Different letters over the bars indicate that the average values differ significantly at a *P* value of <0.05. The experiments shown for panels a and b were repeated twice with essentially the same results.

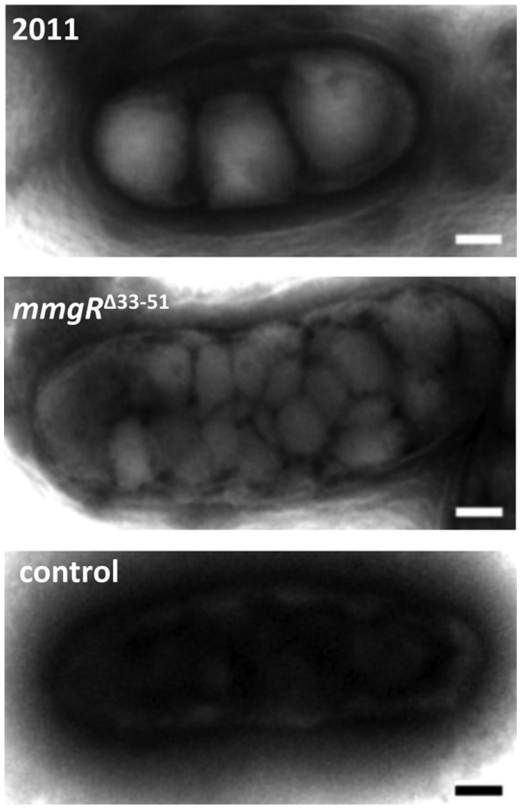

FIG 5 Morphological changes accompanying differential intracellular PHB accumulation. Transmission electron microscopy of wild-type and *mmgR*$^{\Delta 33-51}$ bacteria demonstrated that under conditions of C/N overbalance, stationary-phase *mmgR*$^{\Delta 33-51}$ cells are longer and accumulate a higher number of irregularly shaped PHB granules than the wild-type cells do. The control image corresponds to wild-type bacteria during the exponential phase of growth in RDM, when almost no PHB would be expected to be synthesized. The scale bars indicate a length of 0.25 μm.

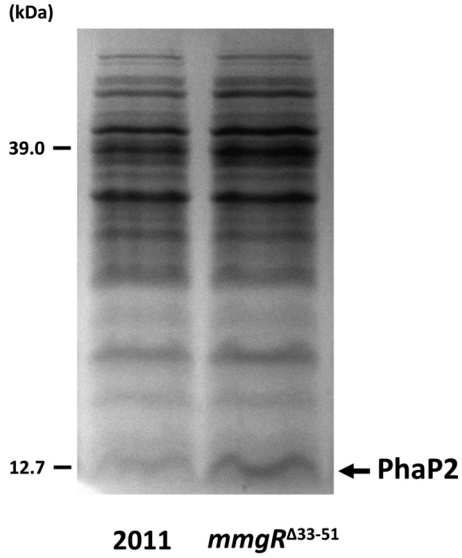

FIG 6 Altered PhaP2 expression in *mmgR*$^{\Delta 33-51}$ mutant cells. SDS-PAGE-based comparative proteomic profiling of the *S. meliloti* 2011 wild-type and *mmgR*$^{\Delta 33-51}$ strains during the stationary phase of growth in RDM is shown. PhaP2 was identified by mass spectrometry (Orbitrap) (see Materials and Methods) as the major protein component of the material extracted from the band indicated with an arrow. The image shows one representative electrophoretic profile among three repetitions with comparable results. The molecular masses of the reference bands are given on the left side of the image.

low-molecular-weight proteins was clearly overrepresented in the mutant proteome and was therefore excised for protein identification (Fig. 6). The PHB granule-associated protein PhaP2 (SMc02111) was identified as the major protein component of the material extracted from the gel (36).

Evidence of posttranscriptional regulation of phasins PhaP1 and PhaP2. In order to further test the molecular findings reported above, we carried out quantitative and comparative proteomic profiling of the wild-type and mutant strains during the stationary phase of growth in RDM by mass spectrometry after differential metabolic labeling of cellular proteins with a heavy (^{15}N) or light (^{14}N) isotope during growth of the bacteria on medium containing either $^{15}NH_4Cl$ or $^{14}NH_4Cl$, respectively, as the sole nitrogen source. This approach allowed us to confirm in quantitative terms the overaccumulation of the PHB phasin PhaP2 in the mutant strain [i.e., $\log_2$ (*mmgR*$^{\Delta 33-51}$/wild type) $= 1.85 \pm 0.77$] and to further detect similar changes in the relative abundance of the other chromosomally encoded PHB-phasin, PhaP1 (SMc00777) [i.e., $\log_2$ (*mmgR*$^{\Delta 33-51}$/wild type) $= 2.10 \pm 0.28$]. Both proteins are much more abundant in the *mmgR*$^{\Delta 33-51}$ mutant than in the wild-type strain (Fig. 7). The inability to detect PhaP1 by SDS-PAGE might be because this phasin possibly reaches lower cellular amounts than the PhaP2. No other proteomic changes of the same relevance and with an evident functional relationship to PHB metabolism were detected by this quantitative approach. Other polypeptides that accumulated slightly in the *mmgR* mutant [i.e., $\log_2$ (*mmgR*$^{\Delta 33-51}$/wild type) > 1.0] were SMb21630 (a conserved hypothetical protein), SoxA2 (a putative sarcosine-oxidase-alpha subunit), FbpA (an Fe^{3+} ABC transporter), and SMc01140 (a probable σ^{54} modulation protein), whereas the single repressed protein in the *mmgR* mutant strain was NrtA [the periplasmic nitrate binding protein of a nitrate transporter; $\log_2$ (*mmgR*$^{\Delta 33-51}$/wild type) $= -1.27$].

In order to determine whether the differential accumulation of phasins was the result of primary changes at the transcriptional or translational level, the corresponding mRNA concentrations were measured by qRT-PCR assays under the same growth conditions in which PhaP1 and PhaP2 were upregulated in the mutant strain. There were no significant differences between the two strains in the relative abundance of the two mRNAs (Fig. 7). These overall results confirm that MmgR negatively controls, in

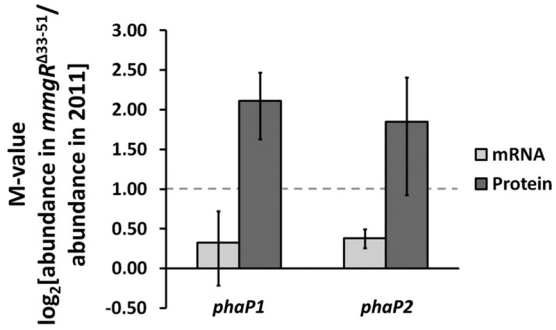

FIG 7 Evidence of posttranscriptional regulation of phasins PhaP1 and PhaP2. The comparative abundances of phasins PhaP1 and PhaP2 and their corresponding mRNAs between the *S. meliloti* 2011 wild-type and *mmgR*$^{\Delta 33-51}$ strains during the stationary phase of growth in RDM are shown. The results are expressed as the average for three biological replicates ± SD. The dashed line indicates the threshold of the M value that was set to consider a certain protein or mRNA as overexpressed in the mutant strain.

a direct or indirect manner, the expression of the phasin genes at a posttranscriptional level.

DISCUSSION

Under conditions of aerobic growth with glucose as the sole C source, *S. meliloti* diverts approximately equal amounts of C to the biosynthesis of balanced cellular biomass in anabolism and to oxidation to CO_2 for energy in catabolism (37). Since the average minimal formula of bacterial biomass is approximated by $C_5H_9O_{2.5}N$ (38), a total C/N molar ratio of 10:1 in a culture medium is expected to be enough to support balanced growth and respiration (i.e., 5 mol of C out of a total of 10 for each mole of N to fuel biomass synthesis, plus another 5 mol for respiration and energy production). In contrast, under an overbalanced C/N ratio (>10:1), the C surplus that is present at the end of the exponential and balanced growth would be expected to be utilized in the synthesis of internal storage compounds, e.g., PHB or glycogen, or of exopolysaccharides that are excreted into the medium (8). The fate of C under such conditions is determined mainly by the current physiological state of the bacterium and as such is subjected to stringent regulation in order to maximize bacterial fitness and well-being (39). Our results demonstrated that when the *mmgR*$^{\Delta 33-51}$ strain (lacking the MmgR transcript) (Fig. 1) grows in RDM with a C/N overbalance of 30:1, that strain produces more biomass and accumulates higher levels of PHB than does the wild type (Fig. 3). This difference suggests that the MmgR transcript negatively controls PHB storage. That the *mmgR* promoter is sharply induced upon cessation of balanced growth because of N depletion regardless of the presence of a C surplus (see Fig. S3 in the supplemental material) suggests that the physiological stimulus promoting *mmgR* expression does not require active PHB synthesis; rather, once *mmgR* is turned on and MmgR accumulates, the fine-tuning capacity of the sRNA becomes manifest under conditions of C/N overbalance so as to regulate PHB synthesis (Fig. 2 to 4). Moreover, we observed that MmgR was able to limit PHB accumulation in the wild-type strain, irrespective of the magnitude of the excess of C in the growth medium (Fig. 4), implying that the MmgR constitutes a tight regulator of PHB storage that serves to set a maximum level of C channeling into the biosynthesis of PHB. Accordingly, the physiological findings were confirmed through direct observation of cells by transmission electron microscopy. The sole absence of MmgR activity in *S. meliloti* had a profound impact on cell morphology during the stationary phase owing to the accumulation of an abnormally high number of irregularly shaped PHB granules (Fig. 5). The higher surface/volume ratio associated with this change in granule number and size distribution suggests that the elevated content of PHB polymer is directly correlated with an increased concentration of phasins that mediate stabilization of the granule-cytoplasm interphase (40).

Complementation with the wild-type *mmgR* allele in *trans* fully restored the growth

phenotype (OD_{600}) and PHB content of the *mmgR*$^{\Delta 33-51}$ mutant strain (Fig. 2 and 3). In contrast, induction of a plasmid-borne *mmgR*$^{\Delta 33-51}$ allele resulted in undetectable levels of the MmgR$^{\Delta 33-51}$ transcript (Fig. 3c), thus suggesting that the internal conserved sequence core of MmgR (Fig. 1) is critical for its stability and therefore for its biological activity. As described elsewhere (41), Hfq is a limiting factor for riboregulatory circuits in bacteria because of competition among sRNAs for accessing Hfq binding sites. To examine the possibility of a side effect of ectopic sRNA induction on the availability of Hfq, we effected overexpression of another Hfq binding sRNA transcript (i.e., Sm84 [25, 27]) and of a small Hfq-independent transcript (asRNA812) (17). Induction of either the Sm84 or the asRNA812 sRNA, however, failed to restore the wild-type ability to limit PHB storage in the *mmgR*$^{\Delta 33-51}$ mutant background under the conditions assayed (Fig. 3b). In conclusion, the inability of all RNAs other than the wild-type *mmgR* to complement the *mmgR*$^{\Delta 33-51}$ mutation demonstrated that the phenotypes associated with the artificial expression of MmgR are specific for this riboregulator and that nonspecific Hfq titration effects could be ruled out. In terms of the symbiotic interaction with the host plant *Medicago sativa* (alfalfa), the *mmgR*$^{\Delta 33-51}$ mutant was Nod$^+$ Fix$^+$ and the symbiotic phenotype was indistinguishable from that of the wild-type parental strain (data not shown). This phenotypic equivalence implies that the loss of negative control over PHB production associated with the lack of MmgR sRNA does not introduce major changes in the symbiotic performance of *S. meliloti*.

S. meliloti has the complete enzymatic machinery to synthesize and degrade intracellular PHB (42). Upon N starvation over a background of C surplus, the production of PHB is turned on as a way to store C and reducing power (42). The production of PHB after growth arrest under saprophytic conditions has been shown to improve the fitness and survival of rhizobial populations during prolonged starvation (43). In addition to the role of PHB as a C storage compound, the possibility of storing reducing power in the form of PHB has been proposed to serve as a buffer to balance the cell's redox state (42). The regulation of PHB accumulation in bacteria has been reported to take place at the transcriptional or enzymatic level or at a combination of both, depending on the species (44). In *S. meliloti*, in addition to the biosynthetic genes *phbAB* and *phbC* and to *phaZ*, the locus encoding the depolymerizing enzyme (42), the formation of PHB granules requires the specific synthesis of the granule-associated phasins PhaP1 and PhaP2 (36), whereas the regulatory protein AniA (PhaR) has been reported to control the flux of C into the alternative polymeric by-products PHB, glycogen, and extracellular polysaccharide (EPS) (12). We have not detected significant differences in the production of extracellular polysaccharide or glycogen (Fig. 3a) in combination with the overproduction of PHB in the *mmgR*$^{\Delta 33-51}$ mutant. A quantitative profiling of the proteomic changes that underlie the *mmgR*$^{\Delta 33-51}$ mutant phenotype during the stationary phase of growth in RDM revealed higher cellular contents of the proteins PhaP1 and PhaP2 in the *mmgR*$^{\Delta 33-51}$ strain (Fig. 6 and 7). The increased abundance of the PhaP1/P2 polypeptides was not, however, accompanied by a comparable increase in their mRNA transcripts (Fig. 7). This finding strongly suggests that an MmgR-dependent posttranscriptional regulatory mechanism operates, either directly or indirectly, on the *phaP1/P2* genes. *In silico* analyses predicted energetically favorable RNA-RNA interactions around the ribosome binding site of both phasin mRNAs and the highly conserved core of the MmgR sRNA (not shown); nevertheless, we cannot rule out the possibility that MmgR targets other mRNAs involved in controlling the flux of C into the synthesis of PHB.

Despite the reported positive role of PHB in multiple metabolic aspects related to the cellular needs for C and energy, it seems reasonable that the accumulation of the polymer and its associated granule proteins has to be limited. Nevertheless, neither the mechanisms nor the regulatory signals by which free-living wild-type *S. meliloti* cells manage to carefully accumulate controlled amounts of PHB within a defined granule architecture have been elucidated. Our results tempt us to speculate that MmgR might be part of a regulatory system that operates to maintain a proper structure and amount of PHB granules through a fine-tuning of the intracellular levels of phasins and polymer,

on the basis of the availability of N and C (the latter relationship is supported by recent and as-yet-unpublished findings from our group). As a result of the mutation in *mmgR*, the loss of that fine adjustment might impair general rhizobial fitness. The negative effects of such a mutation should be investigated under conditions that simulate the natural environment that rhizobia inhabit, which may impose a natural form of selective pressure to preserve this posttranscriptional regulatory mechanism. The results detailed here create new possibilities for a better understanding of the biological significance of PHB dynamics in rhizobia (both in the free-living state and in symbiosis).

The wide distribution of the capacity to synthesize polyhydroxyalkanoates (PHA) observed among eubacterial and archaeal species, along with comparative sequence analyses, has provided extensive evidence for a horizontal genetic flow of structural PHA genes and their corresponding transcriptional regulators (45, 46). The posttranscriptional regulation of PHA (including PHB), however, has been reported in only a single species. In the gammaproteobacterium *Azotobacter vinelandii*, PHB synthesis was previously demonstrated to be under the control of the posttranscriptional regulatory cascade Gac/Rsm (47) and also negatively regulated by the activity of the iron-responsive small RNA ArrF (48–50). The *S. meliloti* genomes, however, lack genetic elements of the Gac/Rsm type (51), and there is no evidence for sequence or structural homology between *A. vinelandii* ArrR and *S. meliloti* MmgR RNAs or their flanking genes. These observations suggest that these two unrelated sRNAs have evolutionarily converged into a common regulation of the same cellular process.

To summarize, our results have demonstrated that the transcript encoded in the *SMc04042-SMc04043* intergenic region of *S. meliloti* 2011 (originally referred to as *sm8*) (Fig. 1) negatively regulates the net metabolic flux of C into the accumulation of the storage polymer PHB. For this reason, we renamed the *sm8* sRNA gene *mmgR*, i.e., a regulatory RNA whose mutation results in a strain that makes more PHB granules. In most instances, these regulatory RNAs act to fine-tune cellular processes and so exhibit mild phenotypes after mutation, thus hindering their functional characterization by reverse genetics (52). In this regard, we would like to highlight the unusual observation that a clear-cut phenotype could be identified following the mutation of the *S. meliloti* *mmgR* gene and that complementation experiments conclusively proved that the changed phenotype resulted from an alteration in the activity of the MmgR transcript.

As we have reported recently (33), the occurrence of *mmgR* alleles in alphaproteobacteria correlates well with the capacity to synthesize and store PHB within this bacterial group, thus suggesting a fundamental coevolutionary relationship between the *mmgR* locus and PHB metabolism. Further studies on the functional adaptation of each *mmgR* ortholog to the biology of its corresponding species will help us to understand more comprehensively the biological role within the phylogeny of one of the most ancient and widely distributed sRNA genes in alphaproteobacteria.

MATERIALS AND METHODS

Bacterial strains and culture conditions. The bacterial strains used in this work are listed in Table 1. *Escherichia coli* strains were cultured at 37°C either in nutrient yeast broth (NYB) (nutrient broth, 25 g per liter; yeast extract, 5 g per liter) or in nutritive agar (blood agar base, 40 g per liter; yeast extract, 5 g per liter). *S. meliloti* strains were cultured at 28°C either in tryptone yeast complex medium (TY) (tryptone, 5 g per liter; yeast extract, 3 g per liter; $CaCl_2 \cdot 2H_2O$, 0.7 g per liter [53]) or in *Rhizobium* defined medium (RDM) (sucrose, 5 g per liter; $MgSO_4 \cdot 7H_2O$, 0.25 g per liter; NH_4Cl, 0.32 g per liter; $CaCl_2 \cdot 2H_2O$, 100 mg per liter; anhydrous $FeCl_3$, 6 mg per liter; H_3BO_3, 3 mg per liter; $MnSO_4 \cdot H_2O$, 1.7 mg per liter; $ZnSO_4 \cdot 7H_2O$, 0.3 mg per liter; $NaMoO_4 \cdot 2H_2O$, 0.12 mg per liter; $CoCl_2 \cdot 6H_2O$, 0.065 mg per liter; K_2HPO_4, 1 g per liter; KH_2PO_4, 1 g per liter; biotin, 1 mg per liter; thiamine, 10 mg per liter [adapted from reference 54]). When appropriate, antibiotics were added to culture media at the following concentrations: for *E. coli*, kanamycin at 25 μg per ml and tetracycline at 10 μg per ml and for *S. meliloti*, streptomycin at 400 μg per ml, neomycin at 120 μg per ml, and tetracycline at 5 μg per ml. Bacterial growth was estimated by monitoring the optical density at 600 nm of culture dilutions made after washing and resuspending cells in an appropriate volume of saline solution (SS) (NaCl, 0.9% [wt/vol]) in order to reach an OD of 0.2 to 0.8. At certain time points during the generation of the curves, viable cell counts were determined (55, 56). The growth assays were repeated at least twice.

Generation of the isogenic *mmgR* mutant and *mmgR*-overexpressing strains. Table 1 summarizes the oligonucleotides and plasmids used in this study. The *S. meliloti* 2011 isogenic *mmgR* mutant ($mmgR^{\Delta 33-51}$) was generated by introduction of a sequence replacement within the conserved core of the

TABLE 1 Bacterial strains, plasmids, and oligonucleotides used in the present work

Strain, plasmid, or oligonucleotide	Genotype, features, or sequence (5′→3′)[a]	Reference or source
Strains		
E. coli		
DH5α	F$^-$ *endA1 hsdR17 supE44 thi-1 recA1 gyrA96 relA1* Δ(*lacZYA-argF*)*U169 deoR* (ϕ80d*lacZ*ΔM15)	58
S17-1 λ*pir*	F$^-$ *pro thi hsdR recA* chromosome::RP4-2 Tc::Mu Km::Tn*7* Tp^r Sp^r λ*pir*	71
S. meliloti		
2011	Wild-type strain SU47 derivative; Str^r	72
2011 *mmgR*$^{\Delta 33-51}$	2011 *mmgR* mutant	This work
2011RI	2011 *sinR sinI* double mutant	This work
2011RI *mmgR*$^{\Delta 33-51}$	2011 *sinR sinI mmgR*$^{\Delta 33-51}$	This work
2011RI *mmgR*$^{\Delta 33-51}$ p-MmgR	2011RI *mmgR*$^{\Delta 33-51}$ bearing pSRK-MmgR	This work
2011RI *mmgR*$^{\Delta 33-51}$ p-MmgR$^{\Delta 33-51}$	2011RI *mmgR*$^{\Delta 33-51}$ bearing pSRK-MmgR$^{\Delta 33-51}$	This work
2011RI *mmgR*$^{\Delta 33-51}$ p-as812	2011RI *mmgR*$^{\Delta 33-51}$ bearing pSRK-as812	This work
2011RI *mmgR*$^{\Delta 33-51}$ p-Sm84	2011RI *mmgR*$^{\Delta 33-51}$ bearing pSRK-Sm84	This work
2011 p*sm8-gfp*	2011 carrying an integrated unique chromosomal copy of a transcriptional reporter fusion of p*mmgR* to the green fluorescent protein gene	34
Plasmids		
pUC57-*mmgR*$^{\Delta 33-51}$	Cloning vector carrying *mmgR*$^{\Delta 33-51}$ mutant allele; Amp^r	This work
pK18mob::*sacB*	Mobilizable vector and suicide vector in *S. meliloti* used for insertional mutagenesis and positive selection of double recombinants with *sacB*; Km^r	73
pK18mob:*sacB-mmgR*$^{\Delta 33-51}$	pK18mob:*sacB* derivative carrying *mmgR*$^{\Delta 33-51}$ mutant allele for genomic exchange	This work
pSRK-Km	Broad-host-range expression vector pBBR1MCS-2 derivative containing the *lac* promoter; *lacI*^{q} *lacZ*α^+ Km^r	74
pSRK-*sinR* p*sinI*	pSRK-Km derivative with a transcriptional fusion of the *lac* promoter to the *S. meliloti* 2011 *sinR* gene; has an orphan *S. meliloti* 2011 *sinI* promoter	This work
pSRK-MmgR	pSRK-*sinR* p*sinI* derivative bearing a transcriptional fusion of the *sinI* promoter to the DNA sequence corresponding to the MmgR transcript of *S. meliloti* 2011	This work
pSRK-MmgR$^{\Delta 33-51}$	pSRK-*sinR* p*sinI* derivative bearing a transcriptional fusion of the *sinI* promoter to the DNA sequence corresponding to the MmgR$^{\Delta 33-51}$ transcript of *S. meliloti* 2011 *mmgR*$^{\Delta 33-51}$	This work
pSRK-as812	pSRK-*sinR* p*sinI* derivative bearing a transcriptional fusion of the *sinI* promoter to the DNA sequence corresponding to the asRNA812 transcript of *S. meliloti* 2011	30
pSRK-Sm84	pSRK-*sinR* p*sinI* derivative bearing a transcriptional fusion of the *sinI* promoter to the DNA sequence corresponding to the sRNA Sm84 transcript of *S. meliloti* 2011	This work
Oligonucleotides		
extHR*mmgR*Fw	GATATTGCCGTGCTCTTCG (−396, −377)	This work
extHR*mmgR*Rv	GCCCGGACTTCATTATCG (+432, +450)	This work
mmgR$^{1-32}$Fw	CGGAAAGCTGCTCTCAATC (−360, −341)	This work
mmgR$^{1-32}$Rv	CCCAAGGAGGGTATTTGC (+15, +32)	This work
qRTPCR-MmgR-Fw	ACTCGTGGCTGCAAATAC (+4, +22)	This work
qRTPCR-MmgR-Rv	GTCTAGGGAGGAAACACC (+30, +48)	This work
qRTPCR-*phaP1*-Fw	AGACGCATTTTCCCTCTC (+21, +38)	This work
qRTPCR-*phaP1*-Rv	GTAGGCTTCCTTCGACTG (+97, +114)	This work
qRTPCR-*phaP2*-Fw	TACGAAGGCTTCTTCACC (+223, +240)	This work
qRTPCR-*phaP2*-Rv	AGGTCGGCATACATCTCAC (+257, +275)	This work
qRTPCR-*SMc01852*-Fw	CCGACCGGATCGAAATCA (+152, +169)	59
qRTPCR-*SMc01852*-Rv	TCGTGTGCAGGATGCTGATG (+336, +355)	59
TSS-MmgR	GAGCCTGACAGCATCGCTACAGTCACTCGTGGCTGCAAATAC	This work
XbaI-MmgR	ATAGTCTAGACGGCGGCTTCATCACGGAAC	This work
TSS_Sm84_410	GAGCCTGACAGCATCGCTACATTGTCTGAGCATCCGGTCC	This work
XbaI_Sm84	ATAGTCTAGACCTACTTCTTTGAAGGCCGCCTG	This work

[a]The positions between which the oligonucleotides anneal are shown in parentheses.

mmgR gene. Eighteen nucleotides (positions 3046287 to 3046363 of the *S. meliloti* strain 2011 chromosome) were replaced by a DNA fragment containing KpnI and SmaI restriction site sequences (5′-GGT ACCCCCGGG-3′) via homologous recombination and allelic exchange (Fig. 1). To this end, a construct carrying the *mmgR* mutant allele flanked by the corresponding 600-nt DNA fragments located upstream and downstream in the chromosomal *mmgR* target sequence (GenScript, USA) was

synthesized and cloned into the pK18mob:*sacB* vector. The plasmid was transformed into *E. coli* S17-1 and transferred to strain 2011 by conjugation. Single-crossover neomycin-resistant mutants were first selected and further plated onto TY agar supplemented with 5% sucrose. Double-crossover strains were selected by checking the loss of sucrose sensitivity and neomycin resistance. The correct allelic exchange in the *mmgR*$^{\Delta 33-51}$ candidate mutants was verified by PCR amplification of the *mmgR* locus with the extHR*mmgR*Fw/extHR*mmgR*Rv primer pair (listed in Table 1), followed by detection of the corresponding restriction products upon amplicon treatment with KpnI. The *mmgR*$^{\Delta 33-51}$ mutant clones were finally confirmed by sequencing the *mmgR* locus (Macrogen Inc., South Korea).

MmgR, MmgR$^{\Delta 33-51}$, the Hfq-independent asRNA812, or the Hfq-dependent Sm84 (17, 27) sRNA was induced in the *mmgR*$^{\Delta 33-51}$ background by an isopropyl-β-D-thiogalactopyranoside (IPTG)-inducible plasmid expression system based on the *sinR-sinI* regulation that has been previously introduced elsewhere (see Fig. S1 in the supplemental material) (30, 57). In brief, a PCR-generated DNA fragment with the complete sequence of the *S. meliloti* 2011 *sinR* gene followed by the *sinR-sinI* inter-open reading frame (ORF) region was fused to a PCR-amplified DNA fragment containing the sequence of MmgR, MmgR$^{\Delta 33-51}$, or Sm84. Each resulting fragment was cloned into the pSRK-Km vector to obtain the respective plasmids pSRK-MmgR, pSRK-MmgR$^{\Delta 33-51}$, and pSRK-Sm84. Plasmid pSRK-asRNA812 (30) was constructed following the same protocol described above. The sRNA expression plasmids were transferred to the *S. meliloti* double mutant strain 2011RI (*sinR sinI*) carrying the *mmgR*$^{\Delta 33-51}$ allele in order to reduce background expression from the chromosomal *sinI* copy upon overexpression of the plasmid-borne *sinR* copy. The resulting strains were named 2011RI *mmgR*$^{\Delta 33-51}$ p-MmgR, 2011RI *mmgR*$^{\Delta 33-51}$ p-MmgR$^{\Delta 33-51}$, 2011RI *mmgR*$^{\Delta 33-51}$ p-as812, and 2011RI *mmgR*$^{\Delta 33-51}$ p-Sm84 (Table 1).

RNA extraction and purification. Total RNA from the bacterial cells was extracted with acid phenol-guanidinium isothiocyanate (TRIzol, Life Sciences) and chloroform, following the manufacturer's instructions. The RNA was then purified by precipitation with isopropanol. Before reverse transcription, the RNA was treated with DNase I for 1 h at 37°C (Thermo Scientific; 1 U DNase I per μg RNA). DNase I was then inactivated by incubation at 65°C after the addition of 0.1 volume of 50 mM EDTA. The purified RNA was then quantified by UV absorbance (NanoDrop; Thermo Scientific, USA) and the quality of the preparation further assessed by denaturing agarose gel electrophoresis (58).

Northern blot analysis. Northern blot analyses were performed as reported elsewhere (58). Two to five micrograms of total RNA from each sample was initially electrophoresed for 45 min at a constant current (15 mA) in polyacrylamide gels (8.3 M urea, 8% [wt/vol] acrylamide, 0.2% [wt/vol] bisacrylamide in 1× Tris-borate-EDTA [TBE] buffer). With the low-range RNA ladder (Thermo Scientific, USA) serving as a molecular weight marker, the corresponding lane was cut and stained separately with ethidium bromide and the image registered with a UV transilluminator. The remaining gel was electroblotted at 150 mA for 30 min onto a Hybond-N membrane in 1× TBE buffer. After a two washes of the membrane with 2× SSC solution (30 mM sodium citrate, 0.3 M NaCl), the RNA was cross-linked to the membrane by exposure to UV light for 5 min. The membranes were then blocked with prehybridization buffer (50% [wt/vol] formamide, 5× SSC, 50 mM phosphate buffer [pH 7.0], 2% [wt/vol] blocking reagent, 0.1% [wt/vol] *N*-laurylsarcosine, 7% [wt/vol] sodium dodecyl sulfate [SDS]) for 1 h at 43°C in a hybridization oven and then incubated overnight at 43°C with the hybridization buffer containing the specific anti-*mmgR*$^{1-32}$ digoxigenin-labeled double-stranded DNA (dsDNA) probe (previously generated by amplification of the corresponding genomic locus with the *mmgR*$^{1-32}$Fw and *mmgR*$^{1-32}$Rv primers [Table 1]). The hybridized membranes were washed under standard stringent conditions, incubated with an alkaline phosphatase-coupled antidigoxigenin antibody solution, washed with the same buffer, and covered with the Lumiphos chemiluminescent reagent (Lumigen, USA) in the dark at room temperature for 5 min. The membranes were exposed for 5 to 180 min to photographic films and then further developed. The membranes were stripped by two incubations with a boiling 0.1% (wt/vol) SDS solution for 30 min. The prehybridization, hybridization, and developing steps were repeated using an anti-5S rRNA probe in order to provide an indication of total RNA load.

Real-time qRT-PCR assays. Real-time quantitative reverse transcription-PCR (qRT-PCR) was performed with the Kapa SYBR Fast one-step qRT-PCR Universal kit (Kapa Biosystems, USA). Briefly, 50 ng of purified total RNA was retrotranscribed and amplified by means of a gene-specific primer pair at a final concentration of 200 mM in a reaction volume of 8 μl. Table 1 lists the primers used for the reactions. The transcript abundance for each gene of interest was calculated through the use of three biological replicates for each strain or culture condition (each with three technical replicates). qPCRs were carried out with a Bioer 9600 thermal cycler (Bioer, China). To confirm the presence of a single amplification product, a melting curve was determined after each cycling. The uniformly expressed gene *SMc01852* was used to normalize gene expression (59). The baseline of each amplification curve, the mean amplification efficiency, the threshold fluorescence value for each primer pair, and the quantification cycle (C_q) corresponding to each reaction were determined with the LinRegPCR software (60).

Determination of cellular PHB content. The cellular PHB content was determined by flow cytometry after staining cells with the fluorescent dye Nile red. Approximately 5 × 10^6 cells were centrifuged from aliquots of three independent cultures, washed once with phosphate-buffered saline (PBS), and then permeabilized by treatment with 35% (vol/vol) aqueous ethanol for 15 min. The permeabilized cells were then collected by centrifugation, washed again with PBS, and resuspended in 500 μl PBS with 0.04% (wt/vol) Nile red. After 30 min of incubation, the cells were analyzed in a FACSCalibur (Becton Dickinson, USA) flow cytometer with excitation by a 488-nm-wavelength argon laser. The fluorescence emitted by Nile red was recorded in channel FL2 (containing a filter with bandwidth of 585 ± 42 nm). The background fluorescence from the Nile-red-stained bacteria was minimal (61). Forward (FSC)- and side (SSC)-scattered light were also registered for a total number of 100,000 events. Cytometric data

analysis was performed with the FlowJo software (FlowJo, USA). The geometric mean and standard deviation (SD) of the arbitrary fluorescence values for each cell population distribution were determined. Tukey's multiple-comparison test was carried out to determine whether or not the mean amounts of intracellular PHB in the populations subjected to analysis were statistically different. Flow cytometry assays were carried out twice.

Determination of bacterial dry weight. Aliquots of stationary-phase cultures at a defined OD_{600} were centrifuged at 14,000 × *g* for 10 min. After two washes with SS, the pellets were dried at 105°C for 24 h and weighed with an analytical balance. After relativization to viable cell counts that had been previously determined, values were expressed as picograms per cell. Cell pellets obtained from three independent cultures of each strain were analyzed, and the results are expressed as the average bacterial dry weight ± one standard deviation.

TEM of bacteria in liquid cultures. Cells of *S. meliloti* 2011 and its isogenic *mmgR*$^{\Delta 33-51}$ mutant from stationary-phase cultures in RDM were negatively stained with a solution of 2% (wt/vol) uranyl acetate for 5 min and then directly observed at a magnification of ×20,000 with a JEOL/JEM 1200 EX II transmission electron microscope (TEM) at the Microscopy Service of the School of Veterinary Sciences (National University of La Plata, La Plata, Argentina). The dimensions of at least 100 cells were analyzed in digitalized images of each sample.

SDS-PAGE and protein identification by means of MS/MS ion search. Cell pellets were collected by centrifuging 1 ml from each of three independent cultures of the wild-type and *mmgR*$^{\Delta 33-51}$ strains in RDM in the stationary phase of growth. The pellets were resuspended in 200 μl of Laemmli buffer (62) and incubated at 100°C for 10 min. After clearing the lysates by centrifugation at 12,000 × *g* for 5 min, 10 μl of each supernatant was loaded into a 15% (wt/vol) SDS-polyacrylamide gel and the proteins separated by electrophoresis for 3 h (62). The proteins were stained with Coomassie brilliant blue R-250 (63) and digitalized. The proteins from the excised gel bands were reduced, alkylated, and digested with trypsin; the peptides were then separated by reverse-phase nanoscale liquid chromatography (NanoLC) and subjected to mass spectrometry (MS) analysis at the CEQUIBIEM facility (Center of Chemical and Biochemical Studies by Mass Spectrometry, Buenos Aires University) as described elsewhere (64). The protein identity was assigned by tandem MS (MS/MS) ion search of MS/MS signals obtained after higher-energy collisional-dissociation fragmentation of the most intense MS peaks.

Quantitative differential proteomic profiling. The *Sinorhizobium meliloti* 2011 wild-type and *mmgR*$^{\Delta 33-51}$ strains were cultured up to the stationary phase of growth in RDM containing $^{14}NH_4Cl$ or $^{15}NH_4Cl$ as the sole nitrogen source. Three independent cultures of each bacterial population were processed as biological replicates. At the moment of the cell harvesting, aliquots of cultures containing 40 OD units each were mixed with their respective pair for proteomic comparison and cooled on ice before centrifuging to collect cell pellets. Proteins were extracted and separated into the cytosolic and membrane subcellular fractions following the protocol described elsewhere (24). The protein concentration in each fraction was determined by the Bradford colorimetric assay (Bradford protein assay Ready-to-Use; Bio-Rad, USA) (65) with a bovine serum albumin solution as a reference, and the quality was verified by SDS-PAGE (62). The proteins from both fractions were precipitated overnight with 6 volumes of ice-cold acetone and stored as dry pellets. An on-pellet trypsin digestion was performed after pellet resuspension in 50 mM Tris-HCl (pH 8.5) buffer, followed by peptide reduction with dithiothreitol and alkylation with iodoacetamide, as described previously (66). The mass spectrometric analysis of the samples was performed with an Orbitrap Velos Pro mass spectrometer (Thermo Scientific, Germany). An Ultimate nanoscale rapid-separation LC–high-pressure liquid chromatography (nanoRSLC-HPLC) system (Thermo Scientific, Germany), equipped with a custom 20-cm by 75-μm column filled with 1.7-μm C_{18} beads, was connected on line to the mass spectrometer through a Thermo Scientific Nanospray Flex ion source. One microliter of the tryptic digest was injected onto a C_{18} micro-preconcentration column (300 μm [inner diameter] by 5 mm). The automated trapping and desalting of the sample, the separation of the tryptic peptides, and the mass spectrometric analysis were performed as described previously (67). Spectra were loaded into the QuPE server (68) at Bielefeld University (Germany). An initial preprocessing of spectra was performed at the server default settings. The peptide identity was assigned through the use of the *S. meliloti* decoy database at the Mascot search engine (Matrix Science, UK) with the following parameters: enzyme, trypsin with 2 uncleaved sites allowed; peptide tolerance, 10 ppm; allowed precursor mass, ^{12}C; ^{15}N metabolic labeling; tolerance threshold, 0.05; allowed charge states, +2 and + 3; instrument, ESI-TRAP; fixed modifications, carbamidomethyl (C); variable modifications, oxidation (M). A false-discovery-rate (FDR) analysis was performed, and only peptides with an FDR lower than 0.05 were considered further. The intensities of the light and heavy isotopes of each peptide were quantified by the RelEx linear exclusion algorithm (69). *mmgR*$^{\Delta 33-51}$/wild-type protein ratios were calculated as the median of the corresponding peptide ratios. A Student *t* test was performed to assess statistical significance.

SUPPLEMENTAL MATERIAL

Supplemental material for this article may be found at https://doi.org/10.1128/JB.00776-16.

SUPPLEMENTAL FILE 1, PDF file, 0.4 MB.

ACKNOWLEDGMENTS

A.L. and C.V. thank Susana Jurado for assistance with the transmission electron microscopy, Valeria Segatori for facilitation of the FACS assays, and Tina Krieg (Marburg

University, Germany) and Pia Valacco and Silvia Moreno (CEQUIBIEM, University of Buenos Aires, Argentina) for their technical assistance with the mass spectrometer. We thank Donald F. Haggerty for his valuable help in editing the final version of the manuscript.

We declare no conflicts of interest.

This work was supported by the Argentinean National Scientific and Technical Research Council (CONICET), the National Agency for Promotion of Science and Technology (ANPCyT), and Universidad Nacional de Quilmes. A.L. was supported by CONICET and DAAD (German Academic Exchange Service) fellowships. G.C.B. was supported by ANPCyT and CONICET fellowships. C.V. is a researcher of CONICET. A.B. was supported by CRC 987 (German Research Foundation). We acknowledge technical assistance and access to resources supported by BMBF grant FKZ 031A533 within the de.NBI network. The Orbitrap mass analyzer was funded by the Deutsche Forschungsgemeinschaft (DFG grant INST 160/503-1 FUGG).

REFERENCES

1. Sawada H, Kuykendall LD, Young JM. 2003. Changing concepts in the systematics of bacterial nitrogen-fixing legume symbionts. J Gen Appl Microbiol 49:155–179. https://doi.org/10.2323/jgam.49.155.
2. Masson-Boivin C, Giraud E, Perret X, Batut J. 2009. Establishing nitrogen-fixing symbiosis with legumes: how many rhizobium recipes? Trends Microbiol 17:458–466. https://doi.org/10.1016/j.tim.2009.07.004.
3. Roumiantseva ML, Andronov EE, Sharypova LA, Dammann-Kalinowski T, Keller M, Young JP, Simarov BV. 2002. Diversity of *Sinorhizobium meliloti* from the Central Asian Alfalfa Gene Center. Appl Environ Microbiol 68:4694–4697. https://doi.org/10.1128/AEM.68.9.4694-4697.2002.
4. Horvath B, Kondorosi E, John M, Schmidt J, Torok I, Gyorgypal Z, Barabas I, Wieneke U, Schell J, Kondorosi A. 1986. Organization, structure and symbiotic function of *Rhizobium meliloti* nodulation genes determining host specificity for alfalfa. Cell 46:335–343. https://doi.org/10.1016/0092-8674(86)90654-9.
5. Jones KM, Kobayashi H, Davies BW, Taga ME, Walker GC. 2007. How rhizobial symbionts invade plants: the *Sinorhizobium-Medicago* model. Nat Rev Microbiol 5:619–633. https://doi.org/10.1038/nrmicro1705.
6. Downie JA. 2014. Legume nodulation. Curr Biol 24:R184–R190. https://doi.org/10.1016/j.cub.2014.01.028.
7. Prell J, Poole P. 2006. Metabolic changes of rhizobia in legume nodules. Trends Microbiol 14:161–168. https://doi.org/10.1016/j.tim.2006.02.005.
8. Zevenhuizen LP. 1981. Cellular glycogen, beta-1,2,-glucan, poly beta-hydroxybutyric acid and extracellular polysaccharides in fast-growing species of *Rhizobium*. Antonie Van Leeuwenhoek 47:481–497. https://doi.org/10.1007/BF00443236.
9. Wang C, Saldanha M, Sheng X, Shelswell KJ, Walsh KT, Sobral BW, Charles TC. 2007. Roles of poly-3-hydroxybutyrate (PHB) and glycogen in symbiosis of *Sinorhizobium meliloti* with *Medicago* sp. Microbiology 153:388–398. https://doi.org/10.1099/mic.0.29214-0.
10. Encarnacion S, Dunn M, Willms K, Mora J. 1995. Fermentative and aerobic metabolism in *Rhizobium etli*. J Bacteriol 177:3058–3066. https://doi.org/10.1128/jb.177.11.3058-3066.1995.
11. Ratcliff WC, Kadam SV, Denison RF. 2008. Poly-3-hydroxybutyrate (PHB) supports survival and reproduction in starving rhizobia. FEMS Microbiol Ecol 65:391–399. https://doi.org/10.1111/j.1574-6941.2008.00544.x.
12. Povolo S, Casella S. 2000. A critical role for *aniA* in energy-carbon flux and symbiotic nitrogen fixation in *Sinorhizobium meliloti*. Arch Microbiol 174:42–49. https://doi.org/10.1007/s002030000171.
13. Wagner EG, Romby P. 2015. Small RNAs in bacteria and archaea: who they are, what they do, and how they do it. Adv Genet 90:133–208. https://doi.org/10.1016/bs.adgen.2015.05.001.
14. Storz G, Vogel J, Wassarman KM. 2011. Regulation by small RNAs in bacteria: expanding frontiers. Mol Cell 43:880–891. https://doi.org/10.1016/j.molcel.2011.08.022.
15. Del Val C, Rivas E, Torres-Quesada O, Toro N, Jimenez-Zurdo JI. 2007. Identification of differentially expressed small non-coding RNAs in the legume endosymbiont *Sinorhizobium meliloti* by comparative genomics. Mol Microbiol 66:1080–1091. https://doi.org/10.1111/j.1365-2958.2007.05978.x.
16. Schluter JP, Reinkensmeier J, Barnett MJ, Lang C, Krol E, Giegerich R, Long SR, Becker A. 2013. Global mapping of transcription start sites and promoter motifs in the symbiotic alpha-proteobacterium *Sinorhizobium meliloti* 1021. BMC Genomics 14:156. https://doi.org/10.1186/1471-2164-14-156.
17. Schluter JP, Reinkensmeier J, Daschkey S, Evguenieva-Hackenberg E, Janssen S, Janicke S, Becker JD, Giegerich R, Becker A. 2010. A genome-wide survey of sRNAs in the symbiotic nitrogen-fixing alpha-proteobacterium *Sinorhizobium meliloti*. BMC Genomics 11:245. https://doi.org/10.1186/1471-2164-11-245.
18. Ulve VM, Sevin EW, Cheron A, Barloy-Hubler F. 2007. Identification of chromosomal alpha-proteobacterial small RNAs by comparative genome analysis and detection in *Sinorhizobium meliloti* strain 1021. BMC Genomics 8:467. https://doi.org/10.1186/1471-2164-8-467.
19. Valverde C, Livny J, Schluter JP, Reinkensmeier J, Becker A, Parisi G. 2008. Prediction of *Sinorhizobium meliloti* sRNA genes and experimental detection in strain 2011. BMC Genomics 9:416. https://doi.org/10.1186/1471-2164-9-416.
20. Jimenez-Zurdo JI, Valverde C, Becker A. 2013. Insights into the noncoding RNome of nitrogen-fixing endosymbiotic *alpha*-proteobacteria. Mol Plant Microbe Interact 26:160–167. https://doi.org/10.1094/MPMI-07-12-0186-CR.
21. Roux B, Rodde N, Jardinaud MF, Timmers T, Sauviac L, Cottret L, Carrere S, Sallet E, Courcelle E, Moreau S, Debelle F, Capela D, de Carvalho-Niebel F, Gouzy J, Bruand C, Gamas P. 2014. An integrated analysis of plant and bacterial gene expression in symbiotic root nodules using laser-capture microdissection coupled to RNA sequencing. Plant J 77:817–837. https://doi.org/10.1111/tpj.12442.
22. Barra-Bily L, Fontenelle C, Jan G, Flechard M, Trautwetter A, Pandey SP, Walker GC, Blanco C. 2010. Proteomic alterations explain phenotypic changes in *Sinorhizobium meliloti* lacking the RNA chaperone Hfq. J Bacteriol 192:1719–1729. https://doi.org/10.1128/JB.01429-09.
23. Barra-Bily L, Pandey SP, Trautwetter A, Blanco C, Walker GC. 2010. The *Sinorhizobium meliloti* RNA chaperone Hfq mediates symbiosis of *S. meliloti* and alfalfa. J Bacteriol 192:1710–1718. https://doi.org/10.1128/JB.01427-09.
24. Sobrero P, Schluter JP, Lanner U, Schlosser A, Becker A, Valverde C. 2012. Quantitative proteomic analysis of the Hfq-regulon in *Sinorhizobium meliloti* 2011. PLoS One 7:e48494. https://doi.org/10.1371/journal.pone.0048494.
25. Sobrero P, Valverde C. 2011. Evidences of autoregulation of *hfq* expression in *Sinorhizobium meliloti* strain 2011. Arch Microbiol 193:629–639. https://doi.org/10.1007/s00203-011-0701-1.
26. Torres-Quesada O, Oruezabal RI, Peregrina A, Jofre E, Lloret J, Rivilla R, Toro N, Jimenez-Zurdo JI. 2010. The *Sinorhizobium meliloti* RNA chaperone Hfq influences central carbon metabolism and the symbiotic interaction with alfalfa. BMC Microbiol 10:71. https://doi.org/10.1186/1471-2180-10-71.
27. Torres-Quesada O, Reinkensmeier J, Schluter JP, Robledo M, Peregrina A, Giegerich R, Toro N, Becker A, Jimenez-Zurdo JI. 2014. Genome-wide profiling of Hfq-binding RNAs uncovers extensive post-transcriptional

rewiring of major stress response and symbiotic regulons in *Sinorhizobium meliloti*. RNA Biol 11:563–579. https://doi.org/10.4161/rna.28239.
28. Sobrero P, Valverde C. 2012. The bacterial protein Hfq: much more than a mere RNA-binding factor. Crit Rev Microbiol 38:276–299. https://doi.org/10.3109/1040841X.2012.664540.
29. Vogel J, Luisi BF. 2011. Hfq and its constellation of RNA. Nat Rev Microbiol 9:578–589. https://doi.org/10.1038/nrmicro2615.
30. Robledo M, Frage B, Wright PR, Becker A. 2015. A stress-induced small RNA modulates *alpha*-rhizobial cell cycle progression. PLoS Genet 11: e1005153. https://doi.org/10.1371/journal.pgen.1005153.
31. Baumgardt K, Smidova K, Rahn H, Lochnit G, Robledo M, Evguenieva-Hackenberg E. 2015. The stress-related, rhizobial small RNA RcsR1 destabilizes the autoinducer synthase encoding mRNA *sinI* in *Sinorhizobium meliloti*. RNA Biol https://doi.org/10.1080/15476286.2015.1110673.
32. Torres-Quesada O, Millan V, Nisa-Martinez R, Bardou F, Crespi M, Toro N, Jimenez-Zurdo JI. 2013. Independent activity of the homologous small regulatory RNAs AbcR1 and AbcR2 in the legume symbiont *Sinorhizobium meliloti*. PLoS One 8:e68147. https://doi.org/10.1371/journal.pone.0068147.
33. Lagares A, Jr, Roux I, Valverde C. 2016. Phylogenetic distribution and evolutionary pattern of an alpha-proteobacterial small RNA gene that controls polyhydroxybutyrate accumulation in *Sinorhizobium meliloti*. Mol Phylogenet Evol 99:182–193. https://doi.org/10.1016/j.ympev.2016.03.026.
34. Ceizel Borella G, Lagares A, Jr, Valverde C. 2016. Expression of the *Sinorhizobium meliloti* small RNA gene *mmgR* is controlled by the nitrogen source. FEMS Microbiol Lett 363. https://doi.org/10.1093/femsle/fnw069.
35. Koch AL. 1961. Some calculations on the turbidity of mitochondria and bacteria. Biochim Biophys Acta 51:429–441. https://doi.org/10.1016/0006-3002(61)90599-6.
36. Wang C, Sheng X, Equi RC, Trainer MA, Charles TC, Sobral BW. 2007. Influence of the poly-3-hydroxybutyrate (PHB) granule-associated proteins (PhaP1 and PhaP2) on PHB accumulation and symbiotic nitrogen fixation in *Sinorhizobium meliloti* Rm1021. J Bacteriol 189:9050–9056. https://doi.org/10.1128/JB.01190-07.
37. Fuhrer T, Fischer E, Sauer U. 2005. Experimental identification and quantification of glucose metabolism in seven bacterial species. J Bacteriol 187:1581–1590. https://doi.org/10.1128/JB.187.5.1581-1590.2005.
38. Roels JA. 1980. Application of macroscopic principles to microbial metabolism. Biotechnol Bioeng 22:2457–2514. https://doi.org/10.1002/bit.260221202.
39. Chubukov V, Gerosa L, Kochanowski K, Sauer U. 2014. Coordination of microbial metabolism. Nat Rev Microbiol 12:327–340. https://doi.org/10.1038/nrmicro3238.
40. Potter M, Steinbuchel A. 2005. Poly(3-hydroxybutyrate) granule-associated proteins: impacts on poly(3-hydroxybutyrate) synthesis and degradation. Biomacromolecules 6:552–560. https://doi.org/10.1021/bm049401n.
41. Moon K, Gottesman S. 2011. Competition among Hfq-binding small RNAs in *Escherichia coli*. Mol Microbiol 82:1545–1562. https://doi.org/10.1111/j.1365-2958.2011.07907.x.
42. Trainer MA, Charles TC. 2006. The role of PHB metabolism in the symbiosis of rhizobia with legumes. Appl Microbiol Biotechnol 71:377–386. https://doi.org/10.1007/s00253-006-0354-1.
43. Ratcliff WC, Denison RF. 2010. Individual-level bet hedging in the bacterium *Sinorhizobium meliloti*. Curr Biol 20:1740–1744. https://doi.org/10.1016/j.cub.2010.08.036.
44. Kessler B, Witholt B. 2001. Factors involved in the regulatory network of polyhydroxyalkanoate metabolism. J Biotechnol 86:97–104. https://doi.org/10.1016/S0168-1656(00)00404-1.
45. Cai L, Tan D, Aibaidula G, Dong XR, Chen JC, Tian WD, Chen GQ. 2011. Comparative genomics study of polyhydroxyalkanoates (PHA) and ectoine relevant genes from *Halomonas* sp. TD01 revealed extensive horizontal gene transfer events and co-evolutionary relationships. Microb Cell Fact 10:88. https://doi.org/10.1186/1475-2859-10-88.
46. Kalia VC, Lal S, Cheema S. 2007. Insight in to the phylogeny of polyhydroxyalkanoate biosynthesis: horizontal gene transfer. Gene 389:19–26. https://doi.org/10.1016/j.gene.2006.09.010.
47. Hernandez-Eligio A, Moreno S, Castellanos M, Castaneda M, Nunez C, Muriel-Millan LF, Espin G. 2012. RsmA post-transcriptionally controls PhbR expression and polyhydroxybutyrate biosynthesis in *Azotobacter vinelandii*. Microbiology 158:1953–1963. https://doi.org/10.1099/mic.0.059329-0.
48. Muriel-Millan LF, Castellanos M, Hernandez-Eligio JA, Moreno S, Espin G. 2014. Posttranscriptional regulation of PhbR, the transcriptional activator of polyhydroxybutyrate synthesis, by iron and the sRNA ArrF in *Azotobacter vinelandii*. Appl Microbiol Biotechnol 98:2173–2182. https://doi.org/10.1007/s00253-013-5407-7.
49. Pyla R, Kim TJ, Silva JL, Jung YS. 2009. Overproduction of poly-beta-hydroxybutyrate in the *Azotobacter vinelandii* mutant that does not express small RNA ArrF. Appl Microbiol Biotechnol 84:717–724. https://doi.org/10.1007/s00253-009-2002-z.
50. Pyla R, Kim TJ, Silva JL, Jung YS. 2010. Proteome analysis of *Azotobacter vinelandii arrF* mutant that overproduces poly-beta-hydroxybutyrate polymer. Appl Microbiol Biotechnol 88:1343–1354. https://doi.org/10.1007/s00253-010-2852-4.
51. Agaras B, Sobrero P, Valverde C. 2013. A CsrA/RsmA translational regulator gene encoded in the replication region of a *Sinorhizobium meliloti* cryptic plasmid complements *Pseudomonas fluorescens rsmA/E* mutants. Microbiology 159:230–242. https://doi.org/10.1099/mic.0.061614-0.
52. Papenfort K, Vogel J. 2014. Small RNA functions in carbon metabolism and virulence of enteric pathogens. Front Cell Infect Microbiol 4:91. https://doi.org/10.3389/fcimb.2014.00091.
53. Beringer JE. 1974. R factor transfer in *Rhizobium leguminosarum*. J Gen Microbiol 84:188–198.
54. Vincent JM. 1970. A manual for the practical study of root nodule bacteria. Blackwell Scientific Publications, Oxford, UK.
55. Miles AA, Misra SS, Irwin JO. 1938. The estimation of the bactericidal power of the blood. J Hyg (Lond) 38:732–749. https://doi.org/10.1017/S002217240001158X.
56. Herigstad B, Hamilton M, Heersink J. 2001. How to optimize the drop plate method for enumerating bacteria. J Microbiol Methods 44: 121–129. https://doi.org/10.1016/S0167-7012(00)00241-4.
57. McIntosh M, Meyer S, Becker A. 2009. Novel *Sinorhizobium meliloti* quorum sensing positive and negative regulatory feedback mechanisms respond to phosphate availability. Mol Microbiol 74:1238–1256. https://doi.org/10.1111/j.1365-2958.2009.06930.x.
58. Sambrook J, Fritsch EF, Maniatis T. 1989. Molecular cloning: a laboratory manual, 2nd ed. Cold Spring Harbor Laboratory Press, Cold Spring Harbor, NY.
59. Becker A, Berges H, Krol E, Bruand C, Ruberg S, Capela D, Lauber E, Meilhoc E, Ampe F, de Bruijn FJ, Fourment J, Francez-Charlot A, Kahn D, Kuster H, Liebe C, Puhler A, Weidner S, Batut J. 2004. Global changes in gene expression in *Sinorhizobium meliloti* 1021 under microoxic and symbiotic conditions. Mol Plant Microbe Interact 17:292–303. https://doi.org/10.1094/MPMI.2004.17.3.292.
60. Ruijter JM, Ramakers C, Hoogaars WM, Karlen Y, Bakker O, van den Hoff MJ, Moorman AF. 2009. Amplification efficiency: linking baseline and bias in the analysis of quantitative PCR data. Nucleic Acids Res 37:e45. https://doi.org/10.1093/nar/gkp045.
61. Kacmar J, Carlson R, Balogh SJ, Srienc F. 2006. Staining and quantification of poly-3-hydroxybutyrate in *Saccharomyces cerevisiae* and *Cupriavidus necator* cell populations using automated flow cytometry. Cytometry 69A:27–35. https://doi.org/10.1002/cyto.a.20197.
62. Laemmli UK. 1970. Cleavage of structural proteins during the assembly of the head of bacteriophage T4. Nature 227:680–685. https://doi.org/10.1038/227680a0.
63. Syrovy I, Hodny Z. 1991. Staining and quantification of proteins separated by polyacrylamide gel electrophoresis. J Chromatogr 569:175–196. https://doi.org/10.1016/0378-4347(91)80229-6.
64. Belfiore C, Ordonez OF, Farias ME. 2013. Proteomic approach of adaptive response to arsenic stress in Exiguobacterium sp. S17, an extremophile strain isolated from a high-altitude Andean Lake stromatolite. Extremophiles 17:421–431. https://doi.org/10.1007/s00792-013-0523-y.
65. Bradford MM. 1976. A rapid and sensitive method for the quantitation of microgram quantities of protein utilizing the principle of protein-dye binding. Anal Biochem 72:248–254. https://doi.org/10.1016/0003-2697(76)90527-3.
66. Duan X, Young R, Straubinger RM, Page B, Cao J, Wang H, Yu H, Canty JM, Qu J. 2009. A straightforward and highly efficient precipitation/on-pellet digestion procedure coupled with a long gradient nano-LC separation and Orbitrap mass spectrometry for label-free expression profiling of the swine heart mitochondrial proteome. J Proteome Res 8:2838–2850. https://doi.org/10.1021/pr900001t.
67. Jachlewski S, Jachlewski WD, Linne U, Bräsen C, Wingender J, Siebers B. 2015. Isolation of extracellular polymeric substances from biofilms of the

thermoacidophilic archaeon Sulfolobus acidocaldarius. Front Bioeng Biotechnol 3:123. https://doi.org/10.3389/fbioe.2015.00123.
68. Albaum SP, Neuweger H, Franzel B, Lange S, Mertens D, Trotschel C, Wolters D, Kalinowski J, Nattkemper TW, Goesmann A. 2009. Qupe—a rich Internet application to take a step forward in the analysis of mass spectrometry-based quantitative proteomics experiments. Bioinformatics 25:3128–3134. https://doi.org/10.1093/bioinformatics/btp568.
69. MacCoss MJ, Wu CC, Liu H, Sadygov R, Yates JR, 3rd. 2003. A correlation algorithm for the automated quantitative analysis of shotgun proteomics data. Anal Chem 75:6912–6921. https://doi.org/10.1021/ac034790h.
70. Zuker M. 2003. Mfold web server for nucleic acid folding and hybridization prediction. Nucleic Acids Res 31:3406–3415. https://doi.org/10.1093/nar/gkg595.
71. Simon R, Priefer U, Pühler A. 1983. A broad host range mobilization system for *in vivo* genetic engineering: transposon mutagenesis in Gram negative bacteria. Nat Biotechnol 1:784–791. https://doi.org/10.1038/nbt1183-784.
72. Meade HM, Signer ER. 1977. Genetic mapping of *Rhizobium meliloti*. Proc Natl Acad Sci U S A 74:2076–2078. https://doi.org/10.1073/pnas.74.5.2076.
73. Schafer A, Tauch A, Jager W, Kalinowski J, Thierbach G, Puhler A. 1994. Small mobilizable multi-purpose cloning vectors derived from the *Escherichia coli* plasmids pK18 and pK19: selection of defined deletions in the chromosome of *Corynebacterium glutamicum*. Gene 145:69–73. https://doi.org/10.1016/0378-1119(94)90324-7.
74. Khan SR, Gaines J, Roop RM, II, Farrand SK. 2008. Broad-host-range expression vectors with tightly regulated promoters and their use to examine the influence of TraR and TraM expression on Ti plasmid quorum sensing. Appl Environ Microbiol 74:5053–5062. https://doi.org/10.1128/AEM.01098-08.